ISSN: 2634-9221
European Journal of Applied Sciences; Vol. 14 No. 03 (2026) (609-623)
https://doi.org/10.14738/ejas.1403.11856

Synthesis, Spectroscopy, and DFT Studies of Molybdenum (0) complexes Incorporating the (NN'), (NO) & (OO') Chelating Mixed Ligands as Quinoxaline-2,3-dione, 8-hydroxyquinoline, and 2,2'-bipyridine

Somya Faraj Alshwarif[a,b], Salem Eltuhami Ashoor*[a], Lotfi Belkhiric[c,d], Khalifa Abdulsalam Alfallous[b], Amna Qasem Ali[e], Moussa Abrahim Khlifa[e] and Amel Belgasem Ibrahim[f]

(a) Chemistry Department, Faculty of Science, Misurata University, Misurata, Libya. p. Box 12002, Misurata – Libya
(b) Chemistry Department, Faculty of Science, Alasmarya Islamic University, Zliten, Libya
(c) Pharmaceutical Sciences Research Center CRSP, ZAM Ali Mendjeli, Constantine, Algeria
(d) Laboratory of Mathematical and Subatomic Physics LPMS, University of Constantine Frères Mentouri, Constantine 1, 25017, Algeria
(e) Chemistry Department, Faculty of Science, Sebha University, Sebha, Libya
(f) Department of Pharmacology, Faculty of Medicine, University of Zawia, Libya

Contact author: salem-ashoor@misuratau.edu.ly & salem.oxford.ac.uk@gmail.com

Abstract: The complexes with the formulas [Mo(bipy)(QX)$(CO)_2$], [Mo(bipy)(8HQ)$(CO)_2$], and [Mo(bipy)(8HQ)(QX)] (where QX = quinoxaline-2,3-dione; 8HQ = 8-hydroxyquinoline; bipy = 2,2-bipyridine) were synthesized in two steps. First, $Mo(CO)_6$ was reacted with bipy, and then the QX ligand or 8HQ was added. Initial characterization, based on elemental and mass analyses, suggested three potential structures denoted as 1–3. In these structures, the QX, 8HQ, and bipy ligands coordinate with the Mo(0) centers through their C=O, ON, and NN functional groups. Infrared (IR) studies clarified the coordination modes of the ligands, particularly in the carbonyl region of the spectrum. Proton Nuclear Magnetic Resonance (1H NMR) studies in DMSO-d6 exhibited patterns corresponding to the cis-$(bipy)_2$, QX, or 8HQ moiety. The electronic spectra of the complexes were characterized by charge-transfer transitions, including Mo(dπ)→ C=O (π*), Mo(dπ)→ ON (P: SP^2) 8HQ, and Mo(dπ)→bipy(SP^2), reflecting metal-to-ligand charge transfer (MLCT). The structural and vibrational properties, including the energy gap between the highest occupied molecular orbital (HOMO) and the lowest unoccupied molecular orbital (LUMO) for the complexes [Mo(bipy)(QX)$(CO)_2$], [Mo(bipy)(8HQ)$(CO)_2$], and [Mo(bipy)(8HQ)(QX)], were elucidated using Gaussian09 and Amsterdam Density Functional (AMS/ADF) software. This analysis employed parameterized DFT/B3LYP/6-311G* and the B3LYP method with the TZP basis set.

Keywords: quinoxaline-derivatives, Molybdenum Carbonyl complex, Bipyridine, DFT.

INTRODUCTION

The structural composition of group 6 elements has made their identification significant, especially in relation to their reactions with heterogeneous organic compounds and metal carbonyl chemistry [1]. Additionally, the use of group 6 organometallic catalysts as anti-corrosion agents and accelerators in rubber strengthening has expanded into the pharmaceutical industry, particularly in biochemistry [2–7]. Over the last century, Dwyer

and colleagues have explored the biological activity of ruthenium complexes featuring 2,2-bipyridine (bipy) and 1,10-phenanthroline (phen) ligands [8–12]. Notably, some hydrophobic complexes have demonstrated bacteriostatic and bactericidal properties, as well as the ability to inhibit tumor growth [9,10]. More recently, Meggers and his team have developed organo-ruthenium compounds that act as protein kinase inhibitors [13–15].

The stability of transition metal carbonyl complexes, attributed to the presence of carbonyl (CO) ligands, allows them to follow the 18-electron rule [16–18]. Organometallic fragments, clusters, and metal atoms—whether charged or neutral—can bind to carbon monoxide in either a terminal or multiple bridging fashion, resulting in various molecular complexes. The metal-carbonyl bonding involves σ-donation from the occupied 5σ molecular orbital of CO into an empty metal orbital with σ symmetry, as well as π-backbonding from occupied metal orbitals into the π* molecular orbitals of CO [19, 20]. In the mid-1930s, Hieber and colleagues [21, 22] reported the synthesis of molybdenum complexes by thermally replacing carbonyl groups in the $Mo(CO)_6$ complex with bipy, resulting in cis-$[Mo(CO)_4(bipy)]$. Additionally, numerous complexes with the formula $[M(CO)_4L]$ (where M = Cr, Mo, W and L = O, N, S, P) have been synthesized through thermal methods over the past 50 years [23,24].

In this work, we synthesized and characterized three novel molybdenum complexes featuring quinoxaline-2,3-dione (QX), 2,2'-bipyridine (bipy), and 8-hydroxyquinoline (8HQ) moieties. The characterization was conducted using elemental analysis and ^{1}HNMR techniques. These complexes are described as $Mo(CO)_6$ moieties coordinating with QX, bipy, and 8HQ ligands through CO, N, N', and OH, respectively. Additionally, we employed DFT theoretical calculations to predict the most stable structures along the reaction pathways and to explore their electronic structure properties.

EXPERIMENTAL

Molybdenum hexacarbonyl $[Mo(CO)_6]$ was purchased from a-Aldrich. 2,2'-bipyridine (bipy) and 8-hydroxyquinoline (8HQ) were obtained from Alfa-Aesar and Ried-de-Haen, respectively. Oxalic acid ($C_2H_2O_4{\cdot}2H_2O$) and 1,2-phenylenediamine ($C_6H_8N_2$) were sourced from Co.-Inc. The ligand quinoxaline-2,3-dione was synthesized following a reported procedure [16]. All solvents were dried according to standard procedures. Elemental analyses were conducted using a Mikroanalytisches Labor Pascher in Remagen-Bandorf, Germany. Mass spectra were obtained with a GC/MS 689N Agilent Technologies Mass Spectrometer, and ^{1}HNMR spectra were recorded on a Bruker Spector AG 400DPX operating at 400 MHz. Infrared spectra were obtained using a Frontier FT-IR Spectrometer (Perkin Elmer) in the range of 600 to 4000 cm^{-1}, and the results were recorded in JPG format. Electronic absorption spectra were measured with a Cary 60 UV-Visible spectrophotometer (Agilent Technologies) in the range of 200 to 800 nm, with data analysis performed using Excel software. Samples with concentrations ranging from 2 to 6 x 10^4 mol dm^{-3} in DMSO were measured against the solvent in the reference cell.

COMPUTATIONAL DETAILS

The three complexes (**1-3**) were fully optimized in vacuum using the full-electron DFT/B3LYP/6-311G* method implemented in the Gaussian09 program package [25].

Following this pre-optimization, energy decomposition analysis (EDA) single-point calculations were conducted using the Amsterdam Density Functional (ADF) engine, as implemented in the AMS2022.102 software package [26, 16]. For the ADF calculations, the all-electron B3LYP method with the TZP basis set—comprising triple-ζ Slater-type orbitals (STO) augmented by polarization functions was applied to all atoms. To confirm that the optimized structures represent true minima, vibrational analysis based on harmonic frequency approximation was performed using ADF single-point calculations at the same B3LYP/TZP level of theory. The binding energy is regarded as a composite of multiple significant terms based on the Gaussian pre-optimized geometries of the complexes 1-3: Equation 3 provides the Pauli electrostatic or repulsion energy (ΔEPauli), the electrostatic energy (ΔEElstat), the orbital interaction energy (ΔEOrbt), and the dispersion energy (ΔEDisp).

$$\Delta_{Ebind} = \Delta E_{Pauli} + \Delta E_{Elstat} + \Delta E_{Orbt} + \Delta E_{Disp} \quad (3)$$

The nature of metal-ligand interactions was quantitatively analyzed using the energy decomposition analysis (EDA) method developed by 88-Ziegler et al. [27], which is based on the transition-state method developed by Morokuma [28] and offers insights into the balance of the various bonding electronic or electrostatic factors at work between the isolated fragments. The three moieties, i.e., [Mo(bipy) + 8HQ$(CO)_2$], [Mo(bipy) + QX$(CO)_2$], and [Mo(bipy)+ QX(8HQ)], were taken into consideration when performing the fragment computations.

Synthesis of [MO(BIPY)(QX)$(CO)_2$] Complex 1

A solution of bipy (0.089 g, 0.570 mmol) in THF was added to a solution of molybdenum hexacarbonyl (0.150 g, 0.570 mmol) in a Schlenk flask under a nitrogen atmosphere. The resulting solution was stirred at reflux temperature for 30 minutes. Afterward, the light red solution was cooled to room temperature, and a THF solution of QX (0.092 g, 0.570 mmol) was added to the reaction mixture, still under nitrogen. The mixture was then heated to reflux for 15 hours, protected from light. During this time, a green solid product formed and was isolated by filtration. The solid was washed several times with THF, hot petroleum ether, and diethyl ether. It was then dried under vacuum for one day and recrystallized from THF, yielding 0.0693 g of product (26% yield).

Anal. Calc. for $C_{20}H_{14}N_4O_4Mo$ (M.W = 470.07): C, 51.04; H, 2.98 ; N ,11.9

Found: C, 51.28; H, 3.14; N, 12.17%.

Synthesis of [Mo(bipy)(8HQ) $(CO)_2$] Complex 2

Using 8HQ (0.082 g, 0.565 mmol) in place of QX, the [Mo(bipy)(8HQ)$(CO)_2$] complex was created using a similar process to that for [Mo(bipy)(QX)$(CO)_2$] (**1**). After recrystallizing a concentrated solution of the complex from THF, black purple powder of the product was obtained (0.0227g, 10 % yield).

Anal. Calc. for $C_{21}H_{15}N_3O_3Mo$ (M.W = 453.85): C, 55.59; H, 3.30; N, 9.27

Found: C, 55.8; H, 3.43; N, 9.51%.

Synthesis of [Mo(bipy)(QX)(8HQ)] Complex 3

Complex (**3**) was synthesized by combining equimolar amounts of molybdenum hexacarbonyl, 2,2'-bipyridine (bipy), and 8-hydroxyquinoline (8HQ) in a 1:1:1 ratio, specifically 0.150 g (0.570 mmol), 0.089 g (0.570 mmol), and 0.082 g (0.565 mmol), respectively. The complex, [Mo(bipy)(8HQ)$(CO)_2$] (**3**), was obtained using the same method described for complex (1). The final solid was dried under vacuum, yielding 0.1229 g of the product, which corresponds to a 39 % yield after recrystallization from a concentrated THF solution.

Anal. Calc. for $C_{27}H_{21}N_5O_3Mo$ (M.W = 559.92): C, 57.93; H, 3.75; N, 12.5

Found: C, 58.17; H, 3.91; N, 13.78%.

RESULTS AND DISCUSSION

Monomer molybdenum complexes were produced by the thermal reaction of $Mo(CO)_6$ with 2,2-bipyridine and the subsequent addition of 2,3-dione (QX) or (8HQ) ligands. A complex with the general formula [Mo(bipy)(QX)$(CO)_2$] or [Mo(bipy)(8HQ)$(CO)_2$] or [Mo(bipy)(QX)(8HQ)] has been found, according to preliminary characterization of the complex based on elemental analysis data.

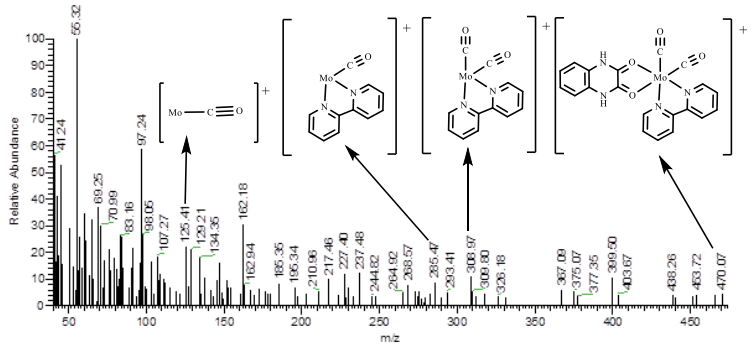

Complexes 1

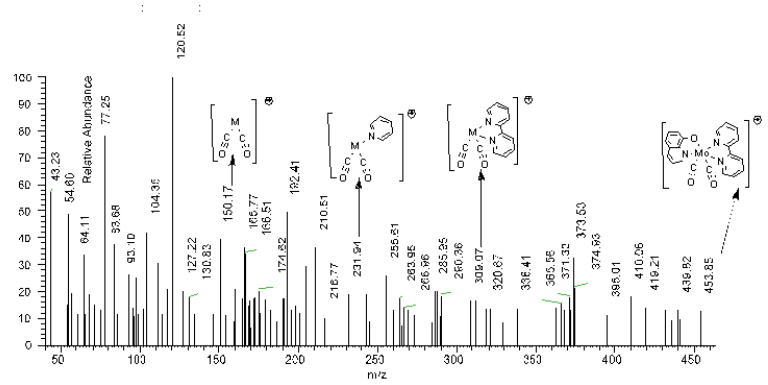

Complexes 2

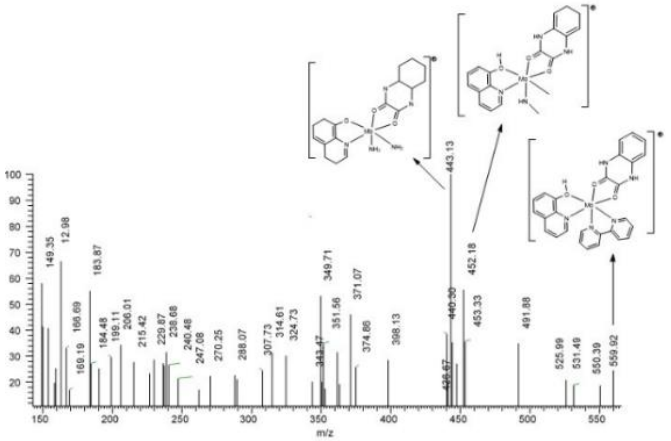

Complexes 3

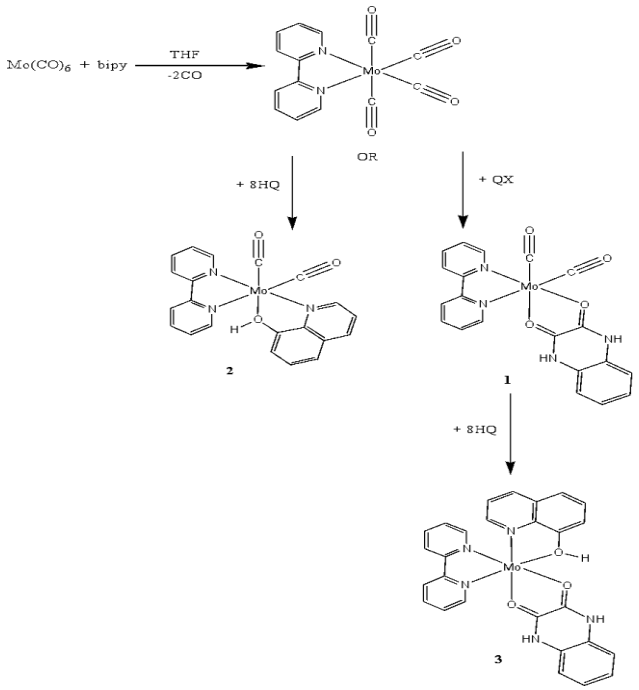

Fig 1: Mass spectra for complexes 1-3

The mass spectra of the molybdenum complexes **1-3**, shown in Fig. 1, exhibited parent peaks due to molecular ions [M]+ at 470.07, 453.45, and 559.92 (m/z) (mass-to-charge ratio) unit, respectively. At 308.97, 231.84, and 452.18, respectively, fragments corresponding to the subsequent fragmentation of the 2,2'-bipyridine, quinoxaline-2,3-dione (QX), and carbonyl CO ligands from the parent complexes were discovered. Three potential structures (**1-3**) for the synthesized complexes depicted in Scheme 1 are suggested by the mass analysis. [Mo(bipy)$(CO)_4$] is created during the reaction's initial phase [18].

Scheme 1: Suggested Structures for the 1-3 Complexes

Recently, Attia and coworkers [18] have shown that group 6 metal carbonyls react with diamines to produce tetracarbonyl products, [$Mo(CO)_4$L] (where L = bipy and DCQX),

significantly enhancing the thermal reactions. The electronic absorption spectrum of molybdenum complexes **1-3**, shown in Fig. 2, is primarily influenced by several metal-to-ligand charge transfer transitions (MCTL) and ligand field (d–d) transitions. The anticipated metal-to-ligand charge transfer transitions include Mo(dπ) → bipy (π*) and Mo(dπ) → CO (π*). It has been reported that the electronic spectrum of complex **1** exhibits an electronic transition at 323 nm, attributed to the M(dπ) → L(p) charge transfer, where L represents either bipy or CO.

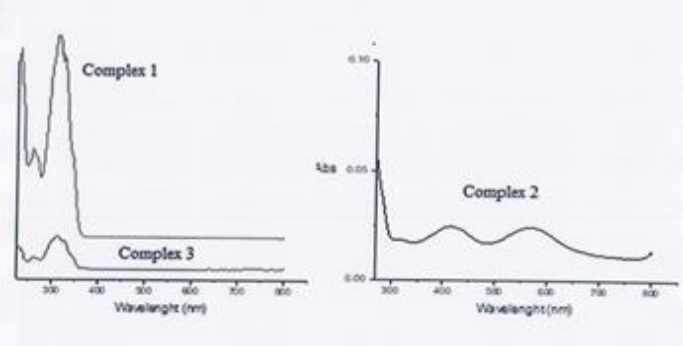

Fig 2: The electronic absorption spectra measured in DMSO for molybdenum complexes 1-3.

Due to two Mo(dπ)→bipy (π*) and Mo(dπ)→CO (π*) electronic transitions, compound 2 exhibits two bands at 415 and 554 nm. The M(dπ)→bipy (π*) charge transfers cause complex **3** to exhibit a single electronic transition at 312 nm. This kind of electronic transition, known as (back bonding), provides the complex with greater stability by transferring an electron from the lowest-energy orbital to the highest-energy orbital, which reduces the buildup of negative charge on the metal. Additionally, the ligand-field transitions (d→d) are not 162-well appearing in any of the complexes under consideration. This is because the strength of the ligand field transition is obscured by the existence of a high-density charge transfer 163-near the area [18, 32].

When quinoxaline-2,3-dione (QX) was added, the [Mo(bipy)$(CO)_4$] molecule's two CO ligands were substituted. The Mo metal then binds to two oxygen atoms of the (QX) ligand to create [Mo(bipy)(QX)$(CO)_2$]. However, by replacing two CO ligands to produce [Mo(bipy)(8HQ)$(CO)_2$], 8-hydroxyquinoline (8HQ) can function as a bidentate ligand and coordinate through its two C=O groups to the Mo metal of [Mo(bipy)$(CO)_4$] molecule. When the two CO groups are positioned in a cis or a trans position around the Mo core, two potential intermediates may arise. Then, as the reaction proceeds, the form of the first step, the separated bipy, from the second step (Scheme 1) may replace two CO of either Mo centers, resulting in complexes 1-3, then add (QX) or 8-hydroxyquinoline (8HQ) molecules by substituting residual two CO ligands forming [Mo(bipy)(QX)(8HQ)] (Scheme 1).

The substitution reactions of [M$(CO)_4$L-L] complexes (M = Cr, Mo, or W and L-L = benzoic acid [1-(Furan-2-yl)methylene] hydrazide (BFMH), benzoic acid [1-(thiophene-2-yl) methylene] hydrazide (BTMH), benzoic acid [1-(thiophene-2-yl)ethylidene] hydrazide (BPMH), and benzoic acid [1-(anisol-3-yl)methylene] hydrazide (BAMH) were reported by Saleem et al. [1]

The predicted structure is described by the infrared spectra of the produced the complexes (1-3) (Scheme 1). In Table 1, the computed (gas phase) and actual (solid state) infrared spectra of complexes 1-3 are reported. Particularly with regard to the bonding of carbonyl complexes, since the carbonyl vibration is free from interaction with other modes and is not hidden by the existence of other vibrations. The amide in complex 1 exhibits absorption bands at 3666 cm^{-1} and 1602 cm^{-1} of the N-H and C=O bonds, respectively, in the infrared spectra of the quinoxaline-2,3-dione (QX) ligand, whereas complex 3 has a faint absorption band at 3048 cm^{-1} and 1668 cm^{-1} for the N-H and C=O bonds, respectively [16].

Table 1: Characteristic calculated and observed vibrational frequencies (cm^{-1}) for the molybdenum complexes 1-3.

Complex 1		**Complex 2**		**Complex 3**		**Assignment**
Calcd	Obsd	Calcd	Obsd	Calcd	Obsd	
3630	3666			3233	3048	v_{asymm} N-H (QX)
1645	1602			1575	1668	vC=O (QX)
1844 & 1797	1678 & 1637	1815 & 1763	1586 & 1570			$v_{symm\ and\ asymm}$ C=O (Carbonyl)
1481	1494	1489	1496	1566	1570	vC=N(bipy)
670	700	720	744			vMo – CO (Carbonyl)
714	719			674	700	v_{asymm} (bipy) N – Mo -O (QX)
		3759	3663	3186	2923	vO-H (8HQ)
		1600	1631	1534	1599	$v_{C=N}$ (8HQ)

The shift of the stretching vibration of the C=N bond at 1494 cm^{-1} in complex **1** can be used to assign the coordination of the 2,2'-bipyridine ligand to the transition metal. The vibrational bands of the C=N bond in complexes 2 and 3 are detected at 1496 cm^{-1} and 1570 cm^{-1}, respectively [18]. The coordination of the 8-hydroxyquinoline ligand to molybdenum metal involves nitrogen and oxygen atoms, resulting in vibrational bands for the O-H and C=N bonds at 3663 cm^{-1} and 1630 cm^{-1} in complex **2**. In complex **3**, the same O-H and C=N bonds are observed at 2923 cm^{-1} and 1599 cm^{-1}, respectively [19].

For complex **1**, the infrared bands were reported to occur at 700 cm^{-1} (Mo-C stretching vibration) and 719 cm^{-1} (QX) O-Mo-N (bipy). On the other hand, complex **2** exhibits absorption bands at 744 cm^{-1} for the Mo–C stretching vibration. Complex **3** showed absorption of the (QX) O-Mo-N(bipy) bond at 700 cm^{-1}. Furthermore, because of their strong back-bonding, complexes **1** and **2** showed two absorption bands in the carbonyl area that corresponded to the two carbonyl stretching frequencies of the cis at 1678 cm^{-1} and 1637 cm^{-1} for complex **1** and 1570 cm^{-1} and 1586 cm^{-1} for complex **2**. They agree with complexes of transition metal carbonyls that have been reported in the literature [18–29, 30].

The ^{1}HNMR spectrum of the complexes illustrated in Fig. 3 effectively reveals the coordination modes of the ligands with molybdenum.

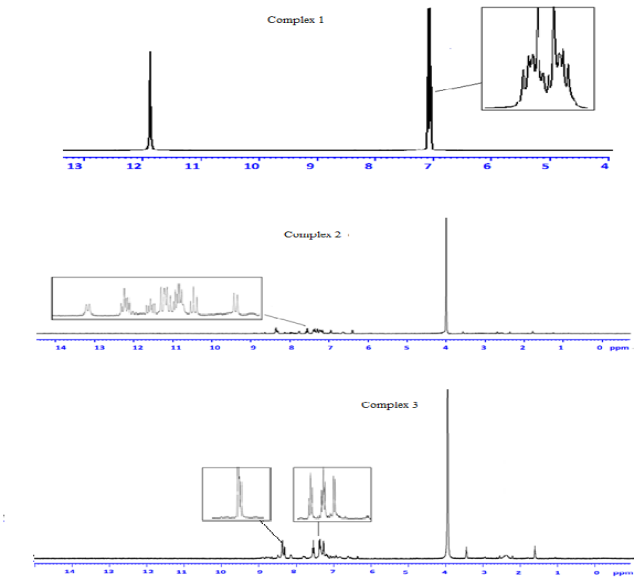

Fig 3: 1H NMR spectrum for 1-3 complexes.

This analysis is particularly useful for assigning the coordination environments of all ligands. Specifically, the chemical shifts for the aromatic quinoxaline-2,3-dione ligand show two peaks at 7.0 and 7.1 ppm in complex **1**, and one peak at 11.9 ppm for the NH proton [16]. In contrast, the 2,2'-bipyridine ligand exhibits four absorption peaks at 7.11 ppm (3H, 3H'), 7.12 ppm (4H, 4H'), 7.13 ppm (5H, 5H'), and one peak at 7.14 ppm (6H, 6H'). Similar behavior is observed in the 1HNMR spectra of complex **1**, with chemical shifts consistent with those reported in the literature [18].

For the 8-hydroxyquinoline ligand, compound 2 displays one observed proton O-H peak at 4 ppm and four observed peaks of the aromatic ring protons at 7, 7.6, 7.7, and 7.95 ppm [31]. The ligand 2,2'-bipyridine was found at 8.5 ppm (3H,3H'), 8.54 ppm (4H,4H'), 8.55 ppm (5H,5H'), and 8.6 ppm (6H,6H') [18]. The 8-hydroxyquinoline ligand shows one signal at 4 ppm for the O-H proton and four peaks at 7.61, 7.62, 7.74, and 7.76 ppm for the aromatic ring protons in the complex 3 instances [31]. The 2,2'-bipyridine ligand exhibits four absorption peaks at 7.78 ppm (3H, 3H'), 8.58 ppm (4H, 4H'), 8.59 ppm (5H, 5H'), and one peak at 8.596 ppm (6H, 6H') [18], as well as two absorption peaks at 7.5 and 7.6 ppm for the aromatic ring protons [16].

Although the mass analysis and infrared spectra are in good accord with the proposed structures **1-3**, no crystals were formed because the synthesized complex lacks structural information. As a result, modeling the three proposed designs using DFT calculations of the most stable structures is thought to be beneficial. The optimal geometry for the most stable structures of complexes **1-3** is depicted in Figure 4.

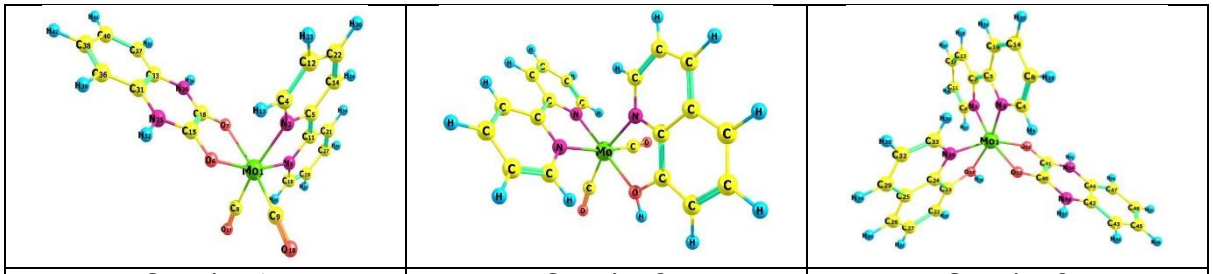

Complex 1	Complex 2	Complex 3

Figure 4: DFT/ZORA/B3LYP/TZP stable structures and labeled geometry of 1-3.

Table 3 reports the calculated bond lengths and angles for **1-3** complexes using the comparative ADF ZORA/B3LYP/TZP and Gaussian (B3LYP/6-311G*) methods. Six coordinating atoms; two O (QX), two N (bipy), and two C (CO) in a deformed octahedral arrangement encircle the core molybdenum metal in complex **1**.

Table 3: Most relevant computed bond lengths (Å) and angles (°) for 1-3 complexes.

Bond lengths	Complex 1		Complex 2		Complex 3	
	ADF	Gaussian	ADF	Gaussian	ADF	Gaussian
Mo1-O1	2.135	2.176	-	-	2.071	2.109
Mo1-O2	2.294	2.359	-	-	2.150	2.199
Mo1-N1	2.191	2.248	2.101	2.176	2.041	2.116
Mo1-N2	2.134	2.162	2.211	2.359	2.081	2.085
Mo1-C3(CO)	1.963	1.968	1.940	2.248	-	-
Mo1-C4(CO)	1.932	1.995	1.951	2.162	-	-
Mo1-O3	-	-	2.281	1.968	2.230	2.308
Mo1-N3	-	-	2.220	1.995	2.072	2.102
Bond angles						
N1-Mo-N2	74.41	73.2	75.17	74.0	76.67	75.4
O1-Mo-O2	72.11	71.2	-	-	74.69	73.6
C3-Mo-C4	85.81	84.8	85.88	85.8	-	-
O3-Mo1-N3	-	-	71.97	70.3	75.94	74.5

In cis-angle disposition, the average of the C3–Mo–C4 bond angles is 85.8° [21]. As anticipated, the nitrogen, oxygen, and carbon donors chelate around the molybdenum center. The bond length values for Mo–O1 (QX), Mo–O2 (QX), Mo–N1(bipy), Mo–N2(bipy), Mo–C3 (CO), and Mo–C4 (CO) are 2.13, 2.29, 407-2.19, 2.13, 1.96, and 1.93 Å, respectively.

The Mo–N bond is calculated to be shorter than those reported for the Mo–O in the $[Mo(OBut)_2(CO)_2(py)_2]$ complex [22], but the Mo–O and Mo–C bond lengths correlate well with those reported for the Mo–O and Mo–C in the $[(bipy)_2Mo(\mu^2\text{-}\kappa2\text{:}\eta^6\text{-}DCQX)Mo(CO)_3]$ complex [18]. Similar to this, complex **2** is made up of a core molybdenum metal that is coupled to six atoms in a deformed octahedral arrangement: one O (8HQ), three N, and two C (CO). Additionally, the average cis-angle disposition of the computed C3–Mo–C4 bond angle is 85.88° [21].

The nitrogen, oxygen, and carbon donors chelate around the molybdenum center as predicted, with bond length values of 2.28, 2.22, 2.10, 2.21, 1.94, and 1.95 Å for Mo–O3

(8HQ), Mo-N3 (8HQ), Mo–N1(bipy), Mo–N2 (bipy), Mo–C3 (CO), and Mo–C4(CO). The lengths of the Mo-C, Mo-O, and Mo-N bonds are in good agreement with those reported for the Mo-C, Mo-O, and Mo-N bonds in the $[Mo(OBut)_2(CO)_2(py)_2]$ and $[Mo_2(pyphos)_4]$ complexes [22,23]. The complex 3 is made up of six coordination centers, or three O and three N, arranged in a deformed octahedral pattern around a central molybdenum atom. With bond length values of 2.23, 2.07, 2.15, 2.07, 2.04, and 2.08 Å for Mo–O1 (8HQ), Mo–N3 (8HQ), Mo-O2 w(QX), Mo-O3(QX), Mo-N1 (bipy), and Mo-N2 (bipy), respectively, the nitrogen and oxygen donors chelate around the molybdenum center. The Mo-N(8HQ) and Mo-O(QX, 8HQ) bond lengths are in good agreement with those reported for the Mo-N and Mo-O bonds the $[(bipy)2Mo(\mu^2\text{- }\mu\ ^2{:}\eta^6\text{-DCQX})Mo(CO)_3]$ and $[Mo_2(pyphos)_4]$ complexes [18, 23].

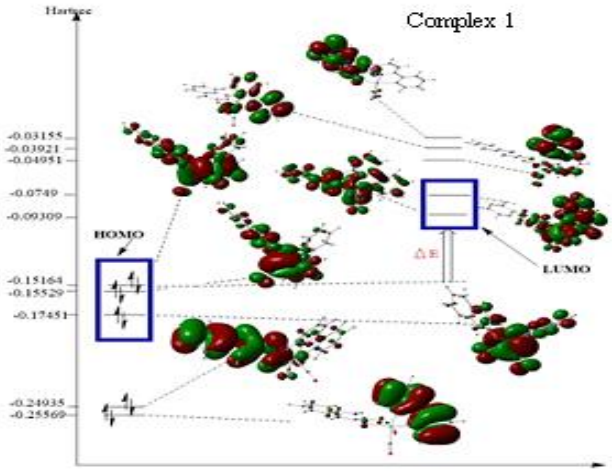

Fig 4: Energy levels, Gap (HOMO - LUMO) and comparing the value of molybdenum complexes 1

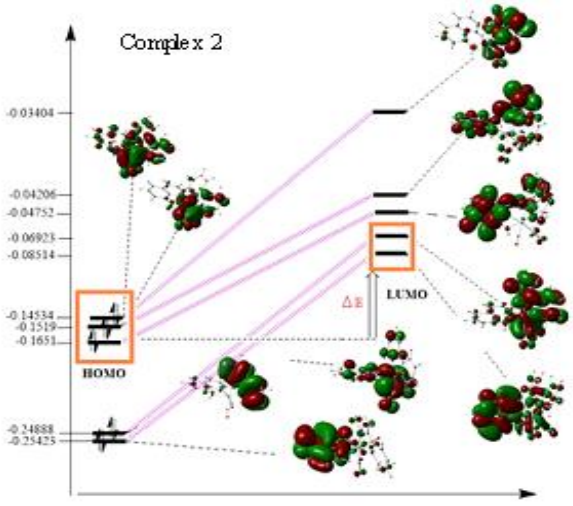

Fig 5: FMO energy levels, Gap (HOMO - LUMO) of molybdenum complex 2

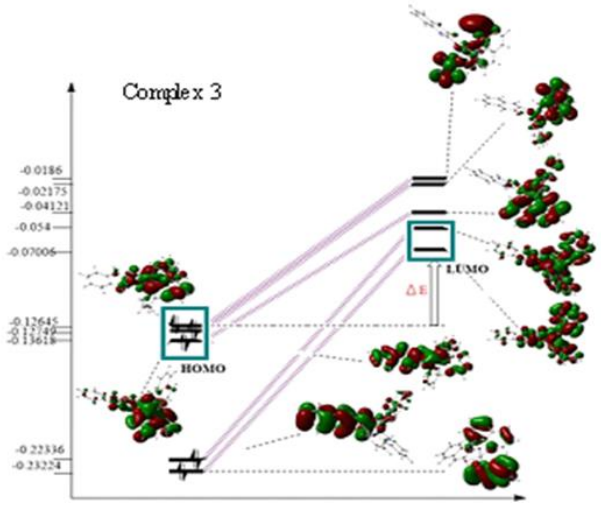

Fig 6: FMO energy levels, Gap (HOMO - LUMO) of molybdenum complex 3

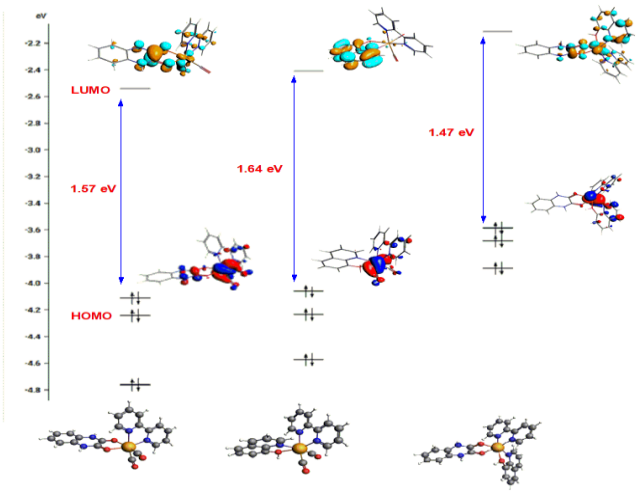

Fig 7: DFT/ZORA/B3LYP/TZP FMO energy levels of molybdenum complexes 1-3

FMO energy levels, gap (HOMO - LUMO) of molybdenum complexes **1-3** are illustrated in Figures 4-6, as well as DFT/ZORA/B3LYP/TZP FMO energy levels in Figure 7. Compared to the 1 and 3 congeners, compound 2 is the most stable, according to FMO energy data (Table 4) of the molybdenum model complexes (**1**-**3**) using the DFT method. In fact, complex 2 is expected to have a greater gap (HOMO-LUMO) than complexes 1 and 3, making it harder and less reactive, as demonstrated by the frontier molecular orbitals (FMO) research [17, 24].

To investigate the evolution of the metallic net charge during ligand-metal donation and retro-donation, the MPA (Mulliken Population Analysis) of the metallic net charge (q) [33] is reported in Table 4. Although MPA has its limitations, it can provide insights into certain aspects of charge transfer and bonding interactions in these complexes. Table 4 shows that the MPA bet charge of metal ion is the lower in complex **1** in comparison to **2**, and **3**, which suggest stronger ligand-metal donation. This also a reminiscence of more pronounced covalent metal-ligand character in complex **1**.

Table 4: Values of HOMO and LUMO for 1-3 complexes.

Transition State	Complex 1	Complex 2	Complex 3
HOMO	-0.151	-0.145	-0.126
LUMO	-0.093	-0.085	-0.070
Hartree	-0.058	-0.060	-0.056
eV	-1.593	-1.638	-1.534
kj/mol	-153.723	-158.055	-148.051
kcal/mol	-36.740	-37.776	-35.385
cm-1	-12850.2	-13212.3	-12376.1
MPA (Mq)	+1.06	+0.99	+1.81

Energy Decomposition Analysis (EDA)

To thoroughly address the metal-ligand covalence, the Energy Decomposition Analysis (EDA) study as well as molecular electrostatic potential (MEP), and atoms-in-molecules (AIM) studies were carried out considering the gas phase (vacuum). To shed more light on the contributions of the different components of the metal−ligand fragment interaction energy ΔEfrag, the following equation is given (see Computational details):

$$\Delta Ef_{rag} = \Delta E_{Pauli} + \Delta ES + \Delta E_{orb} + \Delta E_{disp}$$

Pauli energy repulsion (ΔE_{Pauli}), electrostatic (ΔE_{es}), and covalent steric terms (ΔE_{orb}) are the main decomposition terms (eV), and are reported in Table 5.

Table 5: DFT/B3LYP/TZP EDA (eV) of the complexes 1-3.

Complex	ΔEPauli	ΔEES	ΔEst	ΔEorb	ΔEfrag
Complex 1	20.650	-13.513	7.137	-15.119	-7.982
Complex 2	19.808	-13.221	6.587	-14.422	-7.835
Complex 3	15.764	-11.017	4.747	-10.658	-5.911

As shown by this latter, the destabilizing Pauli term (ΔE_{Pauli}) is computed to be slightly higher for the complex **1** (20.65 eV) than for the complex **2** (19.81 eV), and significantly higher than the complex **3** (15.76 eV). This is traducing the increased steric hindrance caused by the ligands. The stabilizing electrostatic term (ΔE_{ES}) for complexes **1**-**3** is predicted to be significantly high, enhancing their stability. However, it is calculated to be greater for complexes **1** and **2** compared to complex **3**, which aligns with their higher energy levels. Additionally, the steric term (ΔE_{st}) appears to increase in the order of **1** > **2** > **3**. The orbital interaction term (ΔE_{orb}) also plays a substantial role in stabilization, indicating strong charge transfer and polarization interactions within these complexes.

CONCLUSION

Molybdenum (0) Complexes were synthesized and characterized experimentally using spectroscopic methods of types [Mo(bipy)(QX)$(CO)_2$] (**1**), [Mo(bipy)(8HQ)$(CO)_2$] (**2**), and [Mo(bipy)(8HQ)(QX)] (**3**). The ^{1}HNMR spectra of complexes showed the chemical shifts for the organic ligands that attach to the metal center. FMO energy levels and gaps (HOMO -

LUMO) of molybdenum complexes **1**-**3** were illustrated in Figures 4-6, as well as DFT/ZORA/B3LYP/TZP FMO energy levels in Figure 7.

The most stable, according to FMO energy data, was found in compound **2** (Table 4) of the molybdenum model complexes (**1**-**3**) using the DFT method.

Theoretical calculations were performed on complexes **1**, **2** and **3**. Based on the computational studies and physicochemical were discussed, the calculated theoretical geometries showed significant harmony with previous publications. For each complex, an octahedral geometry pattern is proposed around a central molybdenum atom. coordination around the metal ion, which could be due to greater flexibility around the ion metal.

ACKNOWLEDGEMENTS

The main author is grateful to Professor John E. McGrady, an inorganic chemist at Oxford University in England, for allowing me to spend time with his team. Additionally, we are grateful to Mr. Mohamed Alamin and Mrs. Iwona Lall for their support. We express our gratitude to the Chemistry Departments of the Science Faculties at Misurata University and Alasmarya Islamic University, Zliten. The authors are grateful to the Frères Mentouri University of Constantine 1 (Algeria) and the Pharmaceutical Sciences Research Center (CRSP) for providing computing facilities.

REFERENCES

[1] M. Saleem, M. Sharma, S. Mahajan, H. N. Sheikh, and B. L. Kalsotra, “Synthesis and characterization of group-6 metal carbonyl complexes of aroyl hydrazone derivatives,” E-Journal Chem., vol. 9, no. 2, pp. 807–817, 2012. https://doi.org/10.1155/2012/971981

[2] T.-Y. Luh and C. S. Wong, “Transition metal promoted reactions XI. Trimethylamine-N-oxide promoted σ-to π-allyl rearrangement. A convenient synthesis of CpMo (CO) 2 (π-allyl),” J. Organomet. Chem., vol. 287, no. 2, pp. 231–233, 1985. https://doi.org/10.1016/0022-328x(85)87259-4

[3] Y.-K. Au, K.-K. Cheung, and W.-T. Wong, “Synthesis and structural characterization of ruthenium and osmium carbonyl clusters containing 4, 6-dimethylpyrimidine-2-thione,” Inorganica Chim. Acta, vol. 228, no. 2, pp. 267–275, 1995.

[4] P. J. Dyson, “Catalysis by low oxidation state transition metal (carbonyl) clusters,” Coord. Chem. Rev., vol. 248, no. 21–24, pp. 2443–2458, 2004.

[5] P. S. Haddad, G. Miranda, S. R. Ananias, A. E. Mauro, and V. M. Nogueira, “Electrochemical and spectroscopic studies of tungsten carbonyl complexes containing nitrogen and phosphorous ligands,” J. Braz. Chem. Soc., vol. 11, pp. 419–423, 2000.

[6] S. Ghosh et al., “Decarbonylation Reaction of [Os3 (CO) 10 (μ-H)(μ-SN2C4H5)]: X-ray Structures of the Two Isomers of [Os3 (CO) 9 (μ-H)(μ 3-η 2-SN2C4H5)],” J. Chem. Crystallogr., vol. 39, no. 9, pp. 632–637, 2009.

[7] G. Wang and M. Zhou, “Infrared spectra, structures and bonding of binuclear transition metal carbonyl cluster ions,” Chinese J. Chem. Phys., vol. 31, no. 1, pp. 1–11, 2018.

[8] R. Poli, “Open-shell organometallics as a bridge between Werner-type and low-valent organometallic complexes. The effect of the spin state on the stability, reactivity, and structure,” Chem. Rev., vol. 96, no. 6, pp. 2135–2204, 1996.

[9] J. Bohnenberger, W. Feuerstein, D. Himmel, M. Daub, F. Breher, and I. Krossing, “Stable salts of the hexacarbonyl chromium (I) cation and its pentacarbonyl-nitrosyl chromium (I) analogue,” Nat. Commun., vol. 10, no. 1, pp. 1–8, 2019.

[10] G. Frenking, I. Fernández, N. Holzmann, S. Pan, I. Krossing, and M. Zhou, “Metal–CO bonding in mononuclear transition metal carbonyl complexes,” JACS Au, vol. 1, no. 5, pp. 623–645, 2021.

[11] Q. Xu, “Metal carbonyl cations: generation, characterization and catalytic application,” Coord. Chem. Rev., vol. 231, no. 1–2, pp. 83–108, 2002.

[12] L. S. Nogueira et al., “Molybdenum (0) tricarbonyl and tetracarbonyl complexes with a cationic pyrazolylpyridine ligand: synthesis, crystal structures and catalytic performance in olefin epoxidation,” RSC Adv., vol. 8, no. 29, pp. 16294–16302, 2018.

[13] M. H. B. Stiddard, “910. 2, 2′-Bipyridyl derivatives of Group VI carbonyls,” J. Chem. Soc., pp. 4712–4715, 1962.

[14] I. Veroni, C. Makedonas, A. Rontoyianni, and C. A. Mitsopoulou, “An experimental and DFT computational study of a novel zerovalent tetracarbonyl tungsten complex of 2-(2′-pyridyl) quinoxaline,” J. Organomet. Chem., vol. 691, no. 3, pp. 267–281, 2006.

[15] F. A. Cotton, G. Wilkinson, C. A. Murillo, and M. Bochmann, Advanced inorganic chemistry. John Wiley and Sons, Inc., 1999.

[16] Y. Misskire and M. Yohannes, “Synthesis and Characterization of metal complexes of a new heterocyclic Ligand,” Addis Ababa Univ., vol. 1, pp. 1–5, 2006.

[17] S. E. Ashoor, R. A. Abokhater, and N. B. Treina, “Synthesis, DFT Study and the Biological Activity of 8-Hydroxyquinoline Zirconium (IV) Complexes” European Journal of Applied Sciences, Vol. 10 No. 4, pp. 726–737, (2022).

[18] A. S. Attia, A. A. A. Aziz, K. A. Alfallous, and M. F. El-Shahat, “A novel bonding of 6, 7-dichloroquinoxlaine-2, 3-dione, DCQX, to two molybdenum (0) metal centers: Synthesis, characterization, biological activity studies and semiempirical calculations of [(bpy) 2Mo (μ2-κ2: η6-DCQX) Mo (CO) 3] complex,” Polyhedron, vol. 44, no. 1, pp. 238–244, 2012.

[19] C. Zhu, Y. Wang, Q. Mao, F. Li, Y. Li, and C. Chen, “Two 8-Hydroxyquinolinate Based Supramolecular Coordination Compounds: Synthesis, Structures and Spectral Properties,” Materials (Basel)., vol. 10, no. 3, p. 313, 2017.

[20] I. A. Razak, S. Arshad, N. R. Razali, A. A. Rahman, and M. S. M. Yusof, “Structural and Computational Studies of N-[(2 , 6-Diethyl phenyl) carbamothioyl]-2,2-diphenylacetamide , N-[(3Ethylphenyl) carbamothioyl]-2,2-diphenylacetamide and 2,2-Diphenyl-N-{[2-(tri fluoromethyl)phenyl] carbamothioyl } acetamide ,” Int. J. Chem. Mol. Eng., vol. 7, no. 10, pp. 776–784, 2013.

[21] A. Baker, J. Jaud, J.-P. Launay, and J. Bonvoisin, “Structure and spectroscopic studies of cis-bis (bipyridine) ruthenium (II) complexes of phenylcyanamide ligands,” Inorganica Chim. Acta, vol. 358, no. 12, pp. 3513–3518, 2005.

[22] M. H. Chisholm, J. C. Huffman, and R. L. Kelly, “Remarkable influence of terminal alkoxy groups on carbonyl ligands as seen in the new compounds Mo (OBut) 2 (CO) 2 (py) 2 and Mo2 (OPri) 8 (CO) 2,” J. Am. Chem. Soc., vol. 101, no. 25, pp. 7615–7617, 1979.

[23] K. Mashima, H. Nakano, and A. Nakamura, “Reductive Formation of Straight Linear Metal–Metal Bonded Tetranuclear Complexes X– M– Mo– Mo– M– X from X2M…Mo-Mo… MX2 Supported by Four Tridentate 6-Diphenylphosphino-2-pyridonate Ligands (M= Pd, Pt; X= Cl, Br, I),” J. Am. Chem. Soc., vol. 118, no. 38, pp. 9083–9095, 1996.

[24] D. Shoba, S. Periandy, M. Karabacak, and S. Ramalingam, “Vibrational spectroscopy (FT-IR and FT-Raman) investigation, and hybrid computational (HF and DFT) analysis on the structure of 2, 3-naphthalenediol,” Spectrochim. Acta Part A Mol. Biomol. Spectrosc., vol. 83, no. 1, pp. 540–552, 2011.

[25] C. J. Dhanaraj and J. Johnson, “Quinoxaline based bio-active mixed ligand transition metal complexes: Synthesis, characterization, electrochemical, antimicrobial, DNA binding, cleavage, antioxidant and molecular docking studies,” J. Photochem. Photobiol. B Biol., vol. 151, pp. 100–109, 2015.

[26] K. R. Oraby, F. S. M. Hassan, M. A. Zayed, A. E. Mohamed, and I. M. Abdellah, “DFT, TD-DFT and biological activity studies of some maleanilic acid derivatives ligands and their organometallic complexes,” Indian J. Chem. A, vol. 60, no. 12, pp. 1564–1573, 2021.

[27] R. A. Abokhater, S. E. Ashoor, and S. A. Gadir, “Synthesis Spectroscopy and Computational Studies of Manganese (II) Complexes Incorporating (NO)(OO) Ligands and Their Biological Activity”. Asian. J. Appl. Chem. Research ,vol.3 ,no.50157 ,pp. 2582-0273 ,2019.

[28] D. J. Darensbourg, E. B. Frantz, and J. R. Andreatta, “Further studies related to the copolymerization of cyclohexene oxide and carbon dioxide catalyzed by chromium Schiff base complexes. Crystal structures of two μ-hydroxo-bridged Schiff base dimers of chromium (III),” Inorganica Chim. Acta, vol. 360, no. 2, pp. 523–528, 2007.

[29] R. E. Humphrey, "The infrared spectra of aromatic chromium tricarbonyls," Spectrochimica Acta ., vol.17.1, pp. 93-100,1961

[30] R. S. Armstrong, et al. "Infrared and Raman spectra of (η6-C6H6− nXn) Cr (CO) 3 complexes where X= Me (n= 0–6) or OMe (n= 0–2). A study of metal—Ligand interactions," Journal of molecular structure ., vol. 323, pp. 15-28, 1994.

[31] A. J. MARRUGO-GONZÁLEZ, V. D. Orlov, and R. Fernandez-Maestre, “Synthesis of 8-Hydroxyquinoline Chalcones: Trans Configuration, Intramol ecular Hydrogen Bonds, Bromination, and Antifungal Activity,” J. Chil. Chem. Soc., vol. 57, no. 3, pp. 1287–1291, 2012

[32] Kaim, Wolfgang, and Jörg Fees. "The New Tetrafunctional π Acceptor Ligand 3, 6-Bis (2′-pyrimidyl)-1, 2, 4, 5-tetrazine (bmtz): Diruthenium Complexes of bmtz and of its 1, 4-Dihydro Form," Zeitschrift für Naturforschung .,vol. 50.1, pp 123-127,1995.

[33] R.S. Mulliken. "Electronic Population Analysis on LCAO−MO Molecular Wave Functions", "I. J. Chem. Phys".,vol. 23, pp. 1833 −1840, 1955.